Cooling System Pipeline Corrosion Behavior after Reusing of Reverse Osmosis Reject Plant Water as Feed Water Source

A.M.Negm[1]*, A.S. Fouda[2], S.M. Abdelwahab[3], Teraze Albert Youssef[3] and R. Shalof[2]

[1]*Cairo Electricity Production Company, 6th of October, Al Giza, Egypt.*
[2]*Chemistry Department, Faculty of Science, Mansoura University, El-Mansoura, Egypt.*
[3]*Chemistry Department, Faculty of Science, Ain-Shams University, Cairo, Egypt.*

IRON corrosion and wastewater recovery are the most complicated and costly problems facing water utilities. A large number of parameters affect pipe corrosion, including water quality and composition. This work simulated reuse the reject water get out from reverse osmosis desalination plant as feed to cooling system. Evaluation of corrosion rate of pipeline that has been used in cooling system using this water after dosage of new corrosion inhibitors are studied by weight loss, potentiodynamic polarization, electrochemical frequency modulation (EFM) and electrochemical impedance spectroscopy (EIS) methods. The effect of temperature on the corrosion rate was investigated by the weight loss method and some thermodynamic parameters for corrosion and adsorption processes were determined and discussed. The results show that the inhibition efficiency increased with increase in inhibitor concentration and the results obtained from the techniques are in good agreement. The Langelier Saturation Index of the concentrate was reduced from 1.27 (High scale forming) to - 2.27 (No scale forming), thus treated water has properties of low fouling potential that facilitate its recycling and reuse in cooling system.

Keywords: Corrosion Inhibitors; Reverse Osmosis; Reject Water Reuse; Scaling Prevention.

Introduction

Reverse osmosis (RO) is the most widely used method for desalination of brackish water to produce soft water to use it in several industrial applications. This process usually desalinates brackish water having an average Total Dissolved Solids (TDS) and produces desalinated water of less than 5 mg/L TDS and concentrated reject stream of about 4,000 mg/L TDS, depending on the feed water quality and efficiency of the RO plant. Usually RO plants reject 15-20% of the feed water as waste concentrated saline streams that are considered as major environmental and economic drawback of the RO process [1]. RO desalination plants dispose huge amounts of saline waters in many ways that can pollute the neighboring water streams, sewer, and soil surfaces [2,3]. The loss of large part of the feed water in the waste stream is an important challenge and it needs to be separated to increase the overall recovery of the RO plant and to reduce the volume of the reject stream in order to facilitate its disposal in an environmentally acceptable way [4]. As solution for this environmental concern, it is proposed that the produced waste concentrate from the RO unit can be treated to be a suitable feeding source to cooling system. By applying this method, more water recovery will be achieved and the volume of the waste concentrate will be reduced [5].

One of the main obstacles of applying this process is that the waste concentrate produced in RO unit cannot be fed directly to the cooling unit due to the presence of scaling compounds such as calcium (mainly calcium carbonate and calcium sulfate) in large concentrations in the waste concentrate. These compounds cause scaling formation on the pipelines [6] and thus add many operational and economic drawbacks to the process. Scaling is controlled by lowering of pH using a mineral acid. Dosing of hydrochloric acid is the most common method to prevent formation of scaling on pipeline. However, the low pH and presence of high concentration of chloride ions in the concentrate water is the main cause of pipeline corrosion and dosing of suitable corrosion inhibitors is a key parameter to

protect the pipeline and facilitate reuse the waste concentrate.

The use of inhibitors is one of the most practical methods to protect metals against acid attack. Most widely used acid inhibitors are organic compounds containing oxygen, nitrogen and/or sulfur[7]. Hetero-atoms as sulfur, nitrogen and oxygen as well as aromatic rings in their structure are the major adsorption centers that have been adsorbed on the surface of metal. Some works have studied the influence of organic compounds containing nitrogen on the corrosion resistance of steel in acidic media [8-9]most organic inhibitors acting by adsorption on the metal surface. To be effective, an inhibitor must also displace water from the metals surface, to block active corrosion sites and interact with the anodic or cathodic reaction sites to retard the oxidation and/or reduction of corrosion reaction. So, the inhibition efficiency of organic compounds depends on the structure of the inhibitor, the characteristics of the environment, etc…. The main techniques were employed: chemical (weight loss) and electrochemical (potentiodynamic, electrochemical frequency modulation, EFM and electrochemical impedance spectroscopy, EIS). These techniques were performed in 1 M HCl without and with the presence of the investigated compounds in the concentration.

Materials And Experimental Techniques

Composition of the studied specimen
Corrosive solution

A stock solution 5.0 M was prepared from a pure grade of hydrochloric acid and standardized with sodium carbonate solution to determine the concentration of the prepared acid. For our study, 1.0 M HCl aggressive solution was prepared by dilution of the prepared 5.0 M HCl with studied water (RO reject water which has T.D.S nearest to 4000 ppm as Ca_3CO_4).
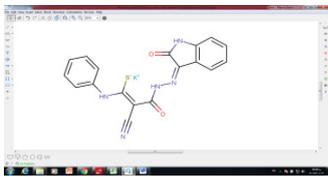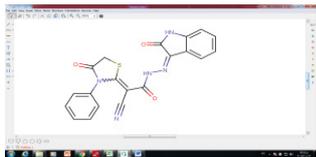
Chemical inhibitor

100 ml stock solutions (10^{-3} M) of compounds (A& B) were prepared by dissolving an accurately weighed quantity of each material in an appropriate volume of absolute ethanol and

TABLE 1. Studied Carbon Steel Composition.

Element	C	Cu	S	Mn	P	Si	Fe
Weight (%)	0.25	0.2	0.05	1.03	0.04	0.28	rest

TABLE 2. The studied compounds structures and molecular weight.

Inhibitor	Structure	Mol. Wt Mol. Formula	IUPAC Name
A		401.49 $C_{18} H_{11} (K^+) N_5 O_2 (S^-)$	potassium [(1Z)-2-cyano-2-{N'-[(3Z)-2-☐oxo-2,3 dihydro-1H-indol-3 ylidene]☐hydrazinecarbonyl}-1 (phenylamino)eth-1-en-1-yl]sulfanide
B		403.42 $C_{20} H_{13} N_5 O_3 S$	2-cyano-N'-[(3Z)-2-oxo-2,3-dihydro-1H-indol-3-ylidene]-2-(4-oxo-3-phenyl-1,3-thiazolidin-2-ylidene)acetohydrazide

dosing the same amount of ethanol to blank to neutralize the ethanol concentration and then the required concentrations (1×10^{-5} - 15×10^{-5}M) were prepared by dilution with studied water.

Measurement techniques

Various techniques have been used for monitoring the corrosion of studied carbon steel in the aggressive solution (1.0 M HCl) with and without the presence of the corrosion inhibitors. These techniques are electrochemical measurements and chemical measurement (weight loss).

Electrochemical techniques

Electrochemical techniques namely, electrochemical impedance spectroscopy (EIS), electrochemical frequency modulation (EFM) and potentiodynamic polarization were utilized in our study to demonstrate the corrosion behavior. In these experiments, typical three chambers glass cell were utilized. It consists of saturated calomel electrode (SCE) as a reference electrode, a platinum blade (1 cm^2) as a counter electrode and carbon steel specimen as working electrode (1 cm^2). The working electrode was polished with several stages of emery paper sizes from 320 to 2000 and then rinsed with deionized water and acetone. The cell was aerated and the measurement was determined at 25 ^{o}C under static conditions. All potential values have been recorded versus saturated calomel electrode.

Tafel curves acquired by altering the potential of the electrode automatically from -900 to -150 mV with consideration of steadystate potential at a scan rate 0.5 mV.S^{-1}. The corrosion potential (E_{corr}) and corrosion current density (i_{corr}) acquired by extrapolation the cathodic and anodic Tafel segments. The *IE* and θ were calculated with the following Equation(1) [10]:

$$IE\,\% = \left(\frac{i^{\circ}_{corr} - i_{corr}}{i^{\circ}_{corr}}\right) x\,100 \;=\; \theta\,x\,100 \quad (1)$$

where, i_{corr} and i°_{corr} are the corrosion current densities in the presence and absence the studied compounds, respectively. By using AC signals, EIS experiments were achieved at a certain corrosion potential in a frequency range of 100 kHz to 100 mHz with capacity of 5 mV peak to peak. The efficiency of the inhibition (IE_{EIS}) obtained using Equation (2) [11]:

$$IE_{EIS}\% = \left(\frac{R_{ct} - R^{\circ}_{ct}}{R_{ct}}\right) x\,100 \;=\; \theta\,x\,100 \quad (2)$$

where, R_{ct} and R°_{ct} are the charge transfer resistance with and without the presence of

studied compounds, respectively. The values of interfacial double layer capacitance (C_{dl}) were acquired by the following Equation(3) [12]:

$$C_{dl} = \frac{1}{2\,\pi\,f_{max}\,R_{ct}} \quad (3)$$

where, f_{max} is the frequency at maximum imaginary component of the impedance. EFM can be achieved as a fast and a nondestructive technique for measurement of corrosion rate. The corrosion current density (i_{corr}), the Tafel slopes (β_a&β_c) and the causality factors (CF-2 & CF-3) can be obtained by the larger peaks. The corrosion inhibition efficiency (*IE*) was calculated according to Equation (1).

By using Gamry Instrument Series (G750^{TM}Potentiostat/Galvanostat/ ZRA with Gamry applications involve EFM 140 software for EFM measurements, DC105 software for potentiodynamic measurements and EIS 300 software for EIS measurements), the electrochemical studies were completed. 5.5 Software of Echem Analyst which put in a computer was used for graphing, plotting and fitting data.

Weight loss technique

Carbon steel specimens with (2.0 - 2.0 - 0.3) cm dimensions were achieved for the chemical method. Before each experiment, the specimens were treated as mentioned in the electrochemical techniques. The coupons immersed in 100 ml beaker after measuring their weights, which contains 100 ml of aggressive solution (RO Reject water plus 1 M HCl) with and without the studied corrosion inhibitors. After various immersion times (30, 60, 90, 120, 150 and 180 min), the carbon steel specimens were pulled out, rinsed with doubly deionized water and reweighted after drying. The surface coverage (θ) and corrosion inhibition efficiency (IE_{wt}) of studied inhibitor have been determined by using the Equation(4) [13]:

$$IE_{wt}\% = (1 - \left(\frac{\Delta W_{inh}}{\Delta W_0}\right)) x\,100 \;=\; \theta\,x\,100 \quad (4)$$

where, ΔW_{inh} and $\Delta W_{\circ}$ are the weight loss of carbon steel with and without the existence of studied compounds, respectively at a specific immersion time (t) and temperature.

Application

Industry is one of the main water users all over the world, accounting for about 40 % of total water abstractions. Water is used in the production

process and is either provided by a public supplier or self-supplied. Furthermore the industrial sector is a major water polluter, as only up to 60 % (value based on data from eight countries) of industrial wastewater receives treatment before being disposed of into the environment. Therefor ethe challenge now how to discover a new source to produce water with specific parameters to share on industrial process and the best way is to desalination of sea and underground water (well & brackish) and reuse to serve industry. Water scientists' methods to desalinate water are ion exchange, thermal methods and reverse osmosis which is the most economical method.

The benefits of reverse osmosis (RO) technology should be well understood in water treatment for sea and brackish water desalination, particularly because of its potential to reduce operating and maintenance expenses. For most sources of water, RO is the least expensive way to remove the majority of dissolved salts.

Osmosis is the process in which water, flows through a semipermeable membrane from a less-concentrated solution to one with a higher concentration. This normal osmotic flow can be reversed (reverse osmosis) by applying hydraulic pressure to the more concentrated (contaminated) solution to produce purified water.

The term total dissolved solids (TDS) refers to mostly inorganic salts present in solution. The salts exist as cations mostly calcium, magnesium, sodium and potassium these cations that cause scaling phenomena for pipeline that pass through and anions mostly bicarbonate, chloride, sulfate, and nitrate these anions especially chloride causes aggressive corrosion for pipeline.

The RO technology is widely used and accepted as it removes both dissolved cations and anions but one of the disadvantages of reverse osmosis philosophy is useless of high concentrated TDS water which called reject water, so this work will focus on the reusing of reject water that gets out from RO plant in cooling system. The very important thing in cooling systems is to protect the pipeline from corrosion and scale formation. The designers should be considered to improve performance and protect plant components to increase the efficiency and life time of systems, so we should eliminate or minimizing the scaling formation and pipeline corrosion of cooling systems.

Water tendency

In cooling systems there are two main goals for the water treatment programs as the following:

• Prevention of salts scaling on pipelines.

• Prevention of pipeline corrosion, these are related but separate issues.

Scale build–up on pipeline, affect operating efficiency and reduce the heat exchanging rate. In the other hand corrosion will reduce the service life of the framing, sumps, piping, and support systems. The studied water source is rejected water of reverse osmosis plant which has high concentration of salts reaches to 4,000 ppm as Ca_3CO_4 so from operation experience this water have high tendency to corrosion and scaling.

Scaling

Scale formations occur when soluble salts are deposited from the feed water on the cooling system components. The parameters which have been found to be most effective in defining the required chemistry for the feed water in cooling systems are its Scaling indices. These indices indicate the tendency of water to be scaling or corrosive as a function of four following factors:–

1. Temperature

2. Hardness

3. Total alkalinity

4. pH

There are three indices in use:–

• Practical (Puckorius) Stability Index

• Ryznar Stability Index (RSI)

• Langelier Saturation Index (LSI)

Determining of Scaling index

The calculation procedures described in this section are adapted from the corresponding ASTM standards,Scaling indices are calculated using total dissolved solids, (which are not measured directly but are derived from the conductivity), temperature, calcium hardness, total alkalinity and pH of the water, after measuring the specific parameters in feed water then select the opposite numerical factors values from Table 3. After that, obey with numerical factors values on equations (5&6) [14]:

$$pH_{eq} = 1.465 \ (\log(TA) + 4.54) \qquad (5)$$

TABLE 3. Scaling indices factors.

Conductivity		Temperature		Calcium Hardness		Total Alkalinity	
µs/cm	Factor A	Ambient Temp. (F)	Factor B	ppm as CaCO3	Factor C	ppm as CaCO3	Factor D
50 - 300	0.1	50 – 56	2.3	10 – 15	0.7	10-15	1.1
301 - 1001	0.2	58 – 62	2.2	16 – 25	0.9	16 - 25	1.3
1001 - 3000	0.25	64 – 70	2.1	26 – 40	1.1	26 - 40	1.5
3000 - 5000	0.27	72 – 80	2	41 – 70	1.35	41 - 70	1.75
				71 – 100	1.55	71 - 100	1.9
				101 – 140	1.7	101 – 140	2.1
				141 – 200	1.85	141 – 200	2.25
				201 – 250	1.95	201 – 250	2.34
				251 – 300	2.05	251 – 300	2.45
				301 – 350	2.12	301 – 350	2.52
				351 – 400	2.18	351 – 400	2.58
				401 – 450	2.24	401 – 450	2.63
				451 – 500	2.26	451 – 500	2.68

$$pH_s = (9.3) + (A + B) - (C + D) \qquad (6)$$

Obtain values of A, B, C, D and E (pH_{eq}) from Table 3, the factors are defined as the following:

A – Factor for total dissolved solids

B – Factor for temperature

C – Factor for calcium hardness (as ppm CaCO3)

D – Factor for alkalinity (as ppm CaCO3)

TA – denotes total alkalinity

After calculating pH_s & pH_{eq} from the previous equations (5&6) we can easily theoretical measure the scaling indices by using the following equations (6, 7&8)[15]:

$$PSI = 2(pH_s) - pH_{eq} \qquad (7)$$

TABLE 4. Scaling & Corrosion water tendency conditions.

Scaling Index Values		Condition
PSI & RSI	LSI	
3	3	Extreme Scaling
4	2	Very Severe Scaling
5	1	Severe Scaling
5.5	0.5	Moderate Scaling
5.8	0.2	Slight Scaling
6	0	Stable
6.5	-0.2	No Scale, very slightly corrosive/tendency to dissolve scale
7	-0.5	No Scale, slightly corrosive/tendency to dissolve scale
8	-1	No scale, moderately corrosive/tendency to dissolve scale
9	-2	No scale, strongly corrosive/tendency to dissolve scale

$$RSI = 2(pH_s) - pH_{measured} \quad (8)$$
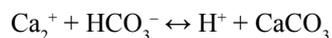
$$LSI = pH_{measured} - pH_s \quad (9)$$

To determine whether the water is scale forming or corrosion formation, and the extent to which it is either according to Table 4. For cooling systems, it is desirable to maintain the water so that it has a slight scale dissolving index. In doing so, the feed water has the ability to dissolve mineral deposits. However, the water should not be so aggressive (corrosion formation) to protect pipelines from deformation.

Control of the Scaling Index by Acid Addition

The factors, which control the scaling index, are interdependent and controlling each of them separately is not possible. For example, changing the hardness, by deionizing, will also affect the alkalinity and pH of the water. Practically the scaling index is set by the chemistry of the feed water and the very effective and cheapest way to prevent the scaling is decrease the scaling index by decrease the pH less than 7 by dosing amount of mineral acids, in the other hand the water becomes very corrosive medium and dissolved the manufacturing material of pipeline which

often made of iron and to overcome this problem we can use corrosion inhibitors which have compatibility with pipeline.

Most natural surface and ground waters are almost saturated with $CaCO_3$. The solubility of $CaCO_3$ depends on the pH, as can be seen from the following equation:

$$Ca_2^+ + HCO_3^- \leftrightarrow H^+ + CaCO_3$$

By adding H^+ as acid, the equilibrium can be shifted to the left side to keep calcium carbonate dissolved. Use food-grade quality acid. Hydrochloric acid is easier to handle and in many countries more readily available than sulfuric acid, however, additional sulfate is added to the feed stream, potentially causing sulfate scaling. $CaCO_3$ tends to dissolve in the concentrate stream rather than precipitate. This tendency can be expressed by the Langelier Saturation Index (LSI) for brackish waters.

Where the methods predicting pH_s are different for LSI and S&DSI as we tabled previously. To control scaling by acid addition alone, the LSI or S&DSI in the concentrate stream must be negative. Acid addition is useful to control scale

TABLE 5. Feed Water Composed Sample Analysis.

Parameter	Value	Unit	Parameter	Value	Unit
pH	7.9	Unit less	CO_3^{-2}	0.05	ppm as CaCO3
Conductivity	5000	µs /cm	Al^{3+}	0	ppm as CaCO3
TDS	4000	ppm as CaCO3	NO_3^-	0	ppm as CaCO3
NH_4^+	0.5	ppm as CaCO3	Cl^-	1517	ppm as CaCO3
K^+	50	ppm as CaCO3	F^-	2.3	ppm as CaCO3
Na^+	910	ppm as CaCO3	SO_4^{2-}	240	ppm as CaCO3
Mg^{2+}	60	ppm as CaCO3	PO_4^{2-}	0	ppm as CaCO3
Ca^{2+}	458	ppm as CaCO3	S^{2-}	0	ppm as CaCO3
Ba^{2+}	0.01	ppm as CaCO3	SiO_2 (colloidal)	2	ppm
Sr^{2+}	3	ppm as CaCO3	SiO_2 (Soluble)	1	ppm
Fe^{2+}	0.1	ppm as CaCO3	Chemical Oxygen Demand	12	ppm
Fe (total)	0.1	ppm as CaCO3	Alkalinity	401	ppm
Mn^{2+}	0	ppm as CaCO3	Total Alkalinity	452	ppm
Boron	1	ppm as CaCO3	Total Organic Carbon	14	ppm
CO_2	5.4	ppm as CaCO3	Avg. Temperature	77	°F

and prevent clogging of pipelines. In the other hand adding of acid may cause severe acidic corrosion of pipeline material and dissolved iron metal and lose the pipelines system so we studied the advantages of dosing of the new corrosion inhibitors (A&B).

Case Study

Feed water analysis: The water samples are taken from RO reject to use it as feed water source to use it in cooling system for gas turbans in 6th of October production electricity plant

Scaling Indices Calculation:

From Table 5.:

Conductivity = 5000 µs/cm

pH$_{measured}$ = 7.9

Temperature = 77 ºF

Calcium Hardness = 458 ppm

Total Alkalinity (TA) = 452 ppm

Alkalinity = 400 ppm

From Table 3.:

A = 0.27

B = 2.0

C = 2.26

D = 2.68

According to equation (5): pH$_{eq}$ = 1.465 (log(TA) + 4.54)

$$pH_{eq} = 1.465 (\log (452) + 4.54)$$

$$pH_{eq} = 1.465 (2.655 + 4.54)$$

$$\textbf{pH}_{\textbf{eq}} \textbf{= 10.54}$$

According to equation (6): pH$_s$ = (9.3) + (A + B) – (C + D)

$$pH_s = 9.3 + (0.27 + 2.0) - (2.26 + 2.68)$$

$$\textbf{pH}_{\textbf{s}} \textbf{= 6.63}$$

According to equation (7): PSI = 2(pH$_s$) – pH$_{eq}$

$$PSI = 2(6.63) – 10.54$$

$$\textbf{PSI = 2.72}$$

According to equation (8): RSI = 2(pH$_s$) – pH$_{measured}$

According to equation (6): pH$_s$ = (9.3) + (A + B) – (C + D)

$$pH_s = 9.3 + (0.27 + 2.0) - (2.26 + 2.68)$$

$$\textbf{pH}_{\textbf{s}} \textbf{= 6.63}$$

$$\textbf{pH}_{\textbf{measured}} \textbf{= 7.9}$$

$$RSI = 2(6.63) – 7.9$$

$$\textbf{RSI = 5.36}$$

According to equation (9): LSI = pH$_{measured}$ – pH$_s$

According to equation (6): pH$_s$ = (9.3) + (A + B) – (C + D)

$$pH_s = 9.3 + (0.27 + 2.0) - (2.26 + 2.68)$$

$$\textbf{pH}_{\textbf{s}} \textbf{= 6.63}$$

$$\textbf{pH}_{\textbf{measured}} \textbf{= 7.9}$$

$$LSI = 7.9 – 6.63$$

$$\textbf{LSI = 1.27}$$

After theoretical calculation of scaling water parameters (RSI, PSI & LSI) the water have extremely scaling tendency.

After dosing of acid with concentration of 1 M:

Conductivity = 5000 µs/cm

pH$_{measured}$ = 4.0

Temperature = 77 ºF

Calcium Hardness = 458 ppm

Total Alkalinity = 452 ppm

Alkalinity = 400 ppm

From Table 3.:

A = 0.27

B = 2.0

C = 2.26

D = 2.68

According to equation (5): pH$_{eq}$ = 1.465 (log(TA) + 4.54)

$$pH_{eq} = 1.465 (\log (452) + 4.54)$$

$$pH_{eq} = 1.465 (2.655 + 4.54)$$

$$\textbf{pH}_{\textbf{eq}} \textbf{= 10.54}$$

According to equation (6): pH$_s$ = (9.3) + (A + B) – (C + D)

$$pH_s = 9.3 + (0.27 + 2.0) - (2.26 + 2.68)$$

pH$_s$ = 6.63

According to equation (7): PSI = 2(pH$_s$) – pH$_{eq}$

PSI = 2(6.63) – 10.54

PSI = 2.72

According to equation (8): RSI = 2(pH$_s$) – pH$_{measured}$

According to equation (6): pH$_s$ = (9.3) + (A + B) – (C + D)

pH$_s$ = 9.3 + (0.27 + 2.0) - (2.26 + 2.68)

pH$_s$ = 6.63

pH$_{measured}$ = 4.0

RSI = 2(6.63) – 4.0

RSI = 13.26 – 4.0

RSI = 9.26

According to equation (9): LSI = pH$_{measured}$ – pH$_s$

According to equation (6): pH$_s$ = (9.3) + (A + B) – (C + D)

pH$_s$ = 9.3 + (0.27 + 2.0) - (2.26 + 2.68)

pH$_s$ = 6.63

pH$_{measured}$ = 4.0

LSI = 4.0 – 6.63

LSI = - 2.27

After dosing of acid and calculation the scale parameters (RSI, PSI & LSI) to verify the results with Table 4., the water tendency scale is changed and the tendency of high salts water shifted from extremely scaling tendency to no scale tendency and ability to dissolved scale but have tendency for corrosion so we tried the derivatives to investigate its ability to work as corrosion inhibitors and studied the corrosion rate and inhibition percentage.

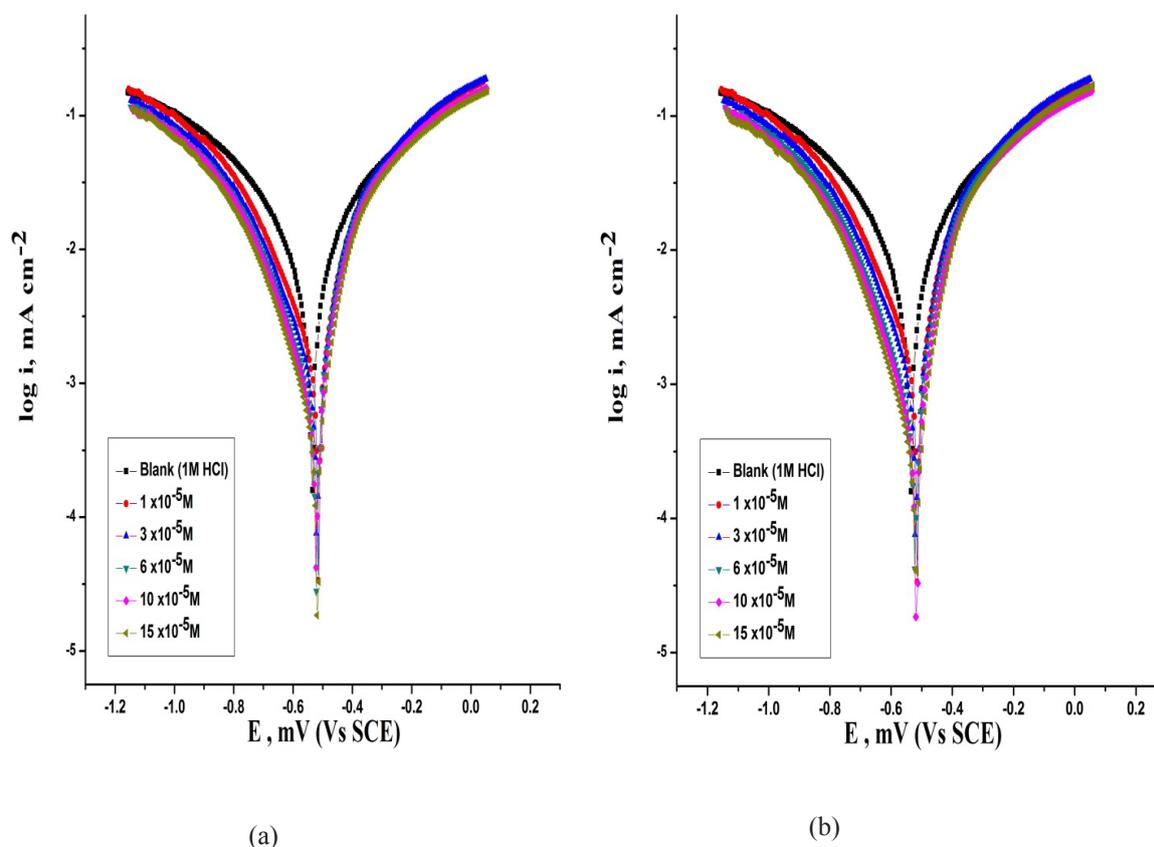(a)   (b)

Fig. 1. Potentiodynamic polarization curves for the corrosion of C-steel in 1 M HCl at 25°C: (a) in the absence and presence of various concentrations of inhibitor (A); (b) in the absence and presence of various concentrations of inhibitor (B).

TABLE 6. Tafel polarization parameters obtained for carbon steel in 1.0 M HCl with and without presence of various concentrations of studied corrosion inhibitors (A&B), at 25 °C.

Compound	Conc., x 10⁻⁵ M	-E$_{corr.}$ mV	i$_{corr.}$ µA cm⁻²	β$_c$ mV dec⁻¹	β$_a$ mV dec⁻¹	Θ	IE_p%
Blank	**1 M HCl**	**511**	**2170.0**	**207**	**205**	**--**	**--**
	1	494	1890.0	262	192	0.129	12.9
	3	492	1050.0	213	145	0.516	51.6
A	6	485	789.0	201	165	0.636	63.6
	10	473	439.0	199	141	0.798	79.8
	15	460	201.0	171	119	0.907	90.7
	1	507	1900.0	257	182	0.124	12.4
	3	504	1130.0	188	136	0.479	47.9
B	6	497	800.0	189	154	0.631	63.1
	10	486	453.0	188	133	0.791	79.1
	15	472	205.0	162	108	0.906	90.6

Results and Discussion

Electrochemical measurements

Potentiodynamic polarization technique

Tafel polarization curves for Carbon steel metal in 1.0 M HCl in the presence and absence of various ratio of investigated compounds (A&B) respectively at 25 °C are shown in Fig. 1. Table 6 listed the Electrochemical parameters such as corrosion current density (i$_{corr}$), Tafel constants (β_a & β_c), corrosion potential (E$_{corr}$), inhibition efficiency (IE_p%) and surface coverage (θ) which obtained from Tafel plots.
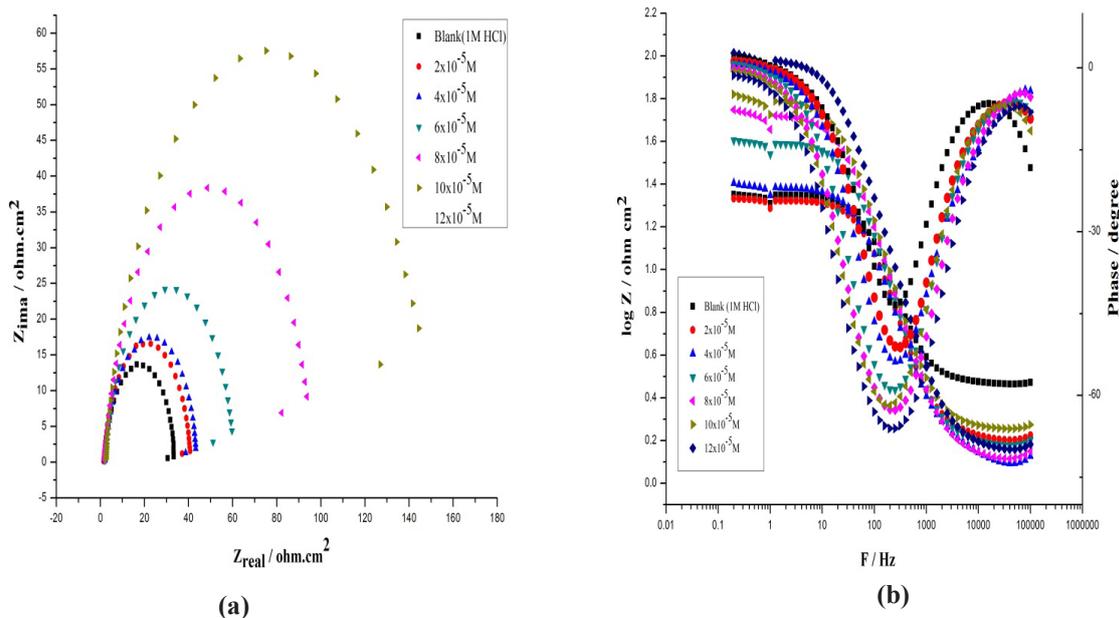

(a)

(b)

Fig. 2. Electrochemical impedance spectroscopy (EIS) plots for the corrosion of C-steel in 1 M HCl in the absence and presence of different concentrations of inhibitor (A) at 25 °C: (a) Nyquist plots; (b) Bode plots.
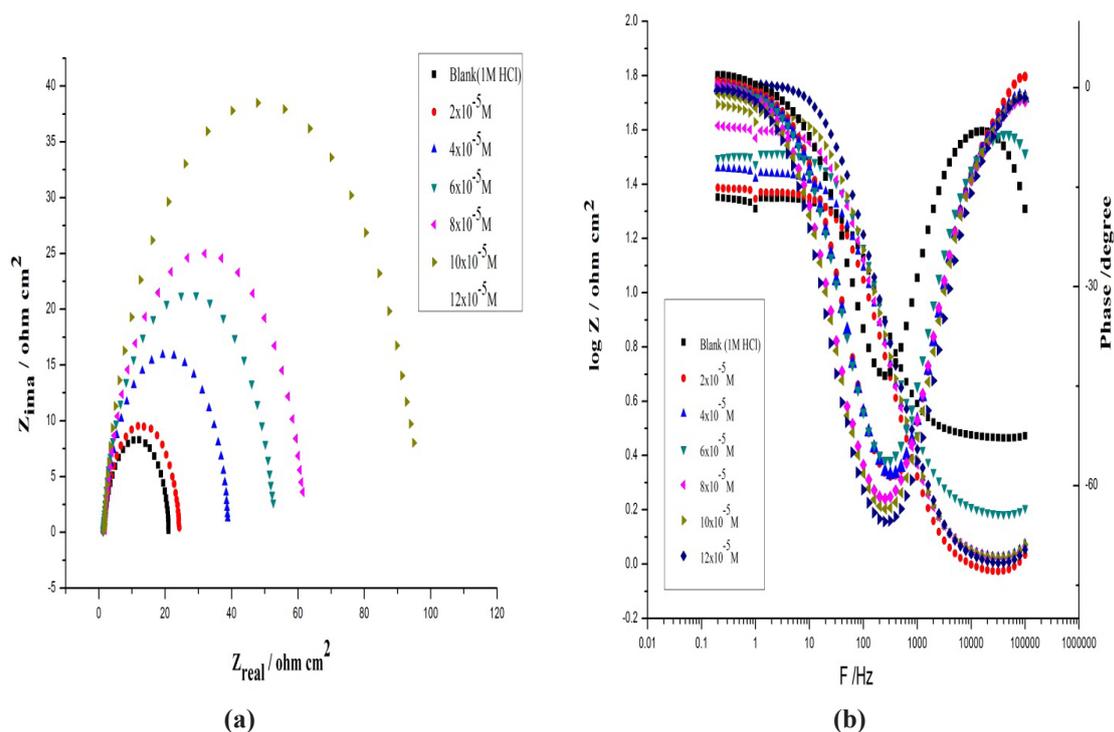
Fig. 3. Electrochemical impedance spectroscopy (EIS) plots for the corrosion of C-steel in 1 M HCl in the absence and presence of different concentrations of inhibitor (B) at 25 °C: (a) Nyquist plots; (b) Bode plots.
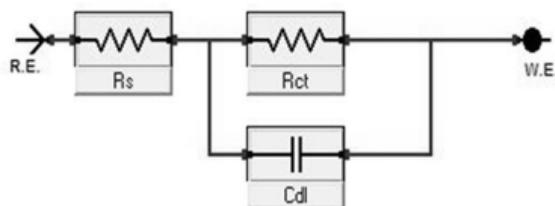

Fig. 4. Electrical equivalent circuit used for modeling the interface carbon steel/ 1.0 M HCl solution without and with studied corrosion inhibitors (A&B).

The results of Table 6 indicate the following:

1. The cathodic and anodic curves obtained exhibit Tafel-type behavior. Addition of investigated derivatives increased both the cathodic and anodic overvoltages and inhibited both the hydrogen evolution and the anodic dissolution processes that are mixed type inhibitors.

2. The corrosion current density (i_{corr}) decreases with increasing the concentration of the investigated derivatives which indicates that these compounds act as inhibitors, and the degree of inhibition depends on the concentration and type of inhibitors present.

3. The slopes of anodic and cathodic Tafel lines (β_a & β_c) were slightly changed by increasing the concentration of the tested compounds. This indicates that these inhibitors act as mixed-type inhibitors. Tafel lines are parallel, which indicates that there is no change of the mechanism of inhibition in the presence and absence of inhibitors. [16].

4. By comparison the inhibition efficiency of two corrosion inhibitors, we found the efficiency of the inhibitor A is higher than second one and this may due to the molecular weight of inhibitor A is higher than the second so it can cover wider surface area so, the results of the investigation show that the inhibiting properties of the derivatives depend on concentration and molecular structure of inhibitor.

TABLE 7. EIS data for dissolution of carbon steel with and without presence of various concentrations of the studied corrosion inhibitors, at 25°C.

Compound	$C_{inh.}$ x10^{-5} M	R_{ct} Ω cm²	C_{dl} μF cm^{-2}	θ	IE_{EIS}%
Blank	1 M HCl	19.4	1.4	--	--
A	1	39.8	1.17	0.513	51.3
	3	41.5	1.09	0.533	53.3
	6	57.7	1.08	0.664	66.4
	10	94	1	0.794	79.4
	15	146.4	0.88	0.868	86.8
B	1	19.7	1.28	0.014	1.4
	3	23.4	1.16	0.172	17.2
	6	51.5	1.11	0.623	62.3
	10	59.9	1.05	0.677	67.7
	15	94.8	0.87	0.796	79.6

Electrochemical impedance spectroscopy (EIS) technique

The plots of Nyquist and Bode are illustrated in Fig. 2 for corrosion inhibitor (A) and Fig. 3 for corrosion inhibitor (B) respectively. The obtained Nyquist represents a single semicircle. Typical circular shape has deviations and these often attributed to the frequency dispersion of interfacial impedance [17]. The Bode plots for the inhibitors are shown in Fig. 2-B, 3-B, where a larger Z_{mod} shows preferable protection for the carbon steel by investigated compounds [18]. Figure 4 illustrates the circuit model used in this experimental test where this circuit applied to analyze the acquired data of impedance. The circuit comprises of the charge-transfer resistance (R_{ct}), the solution resistance (R_s) and double layer capacitance (C_{dl}). Data in Table 7 reveals that the (C_{dl}) value decreases and the (R_{ct}) value increases by raising the concentration of synthesized compounds. This is due to the adsorption of the studied molecules on the Carbon steel surface by the progressive replacement of water molecules [19]. Decreasing the values of (C_{dl}) is assigned to the lowering value of the local dielectric constant and/or the raising of the electrical double layer thickness submitted by studied compounds adsorption on the carbon steel / solution interface [20].

Reasonably good agreement was observed between the values obtained by the electrochemical measurements and the values of inhibition efficiency were in good agreement and the order of *IE%* of these investigated compounds doesn't change and is in the following order:

Compound (A) > Compound (B)

Electrochemical frequency modulation (EFM) technique

EFM is a nondestructive corrosion measurement technique that can directly and quickly determine the corrosion current values without prior knowledge of Tafel slopes and with only a small polarizing signal. These advantages of EFM technique make it an ideal candidate for online corrosion monitoring [21]. The great strength of the EFM is the causality factors which serve as an internal check on the validity of EFM measurement. The causality factors CF-2 and CF-3 are calculated from the frequency spectrum of the current responses.

Figure 5 shows the EFM intermodulation spectra (current versus frequency) of carbon steel in HCl solution containing different concentrations of compound (A). Similar curves were obtained for compounds (B) (not shown).
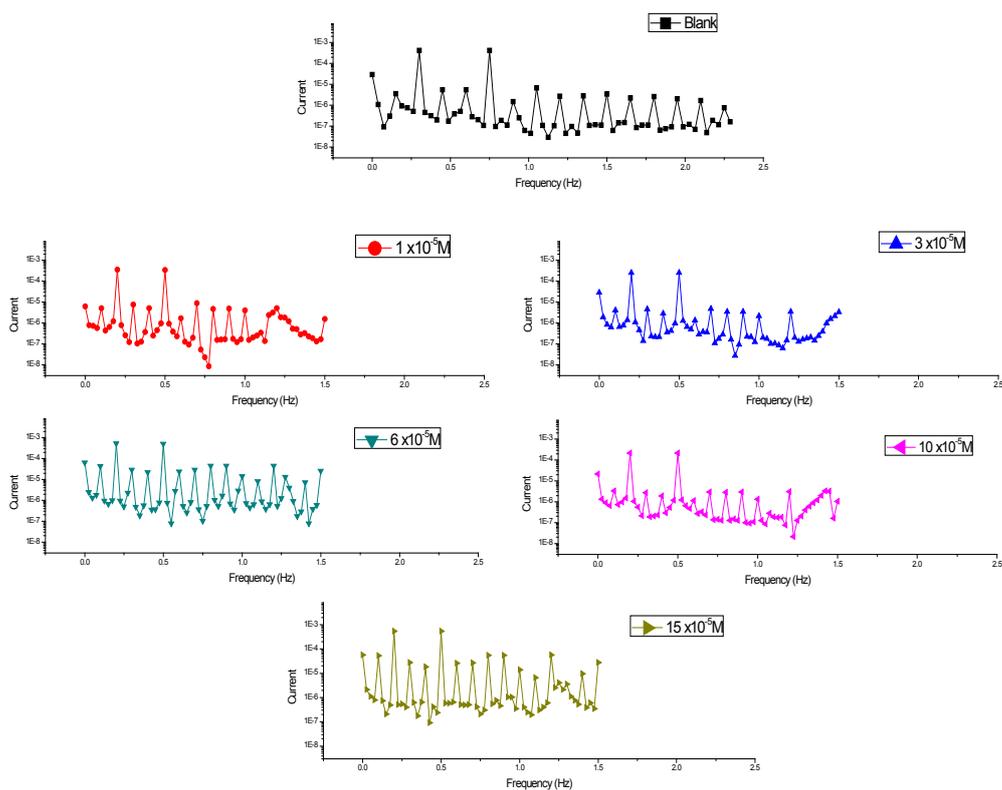
Fig. 5. EFM spectra for carbon steel dissolution with and without presence of different concentrations of investigated inhibitor (A) in 1.0 M HCl, at 25 °C.

TABLE 8. Parameters of electrochemical kinetic acquired by EFM technique for C- steel in 1.0 M HCl with and without presence of various concentrations of inhibitor (A) at 25 °C.

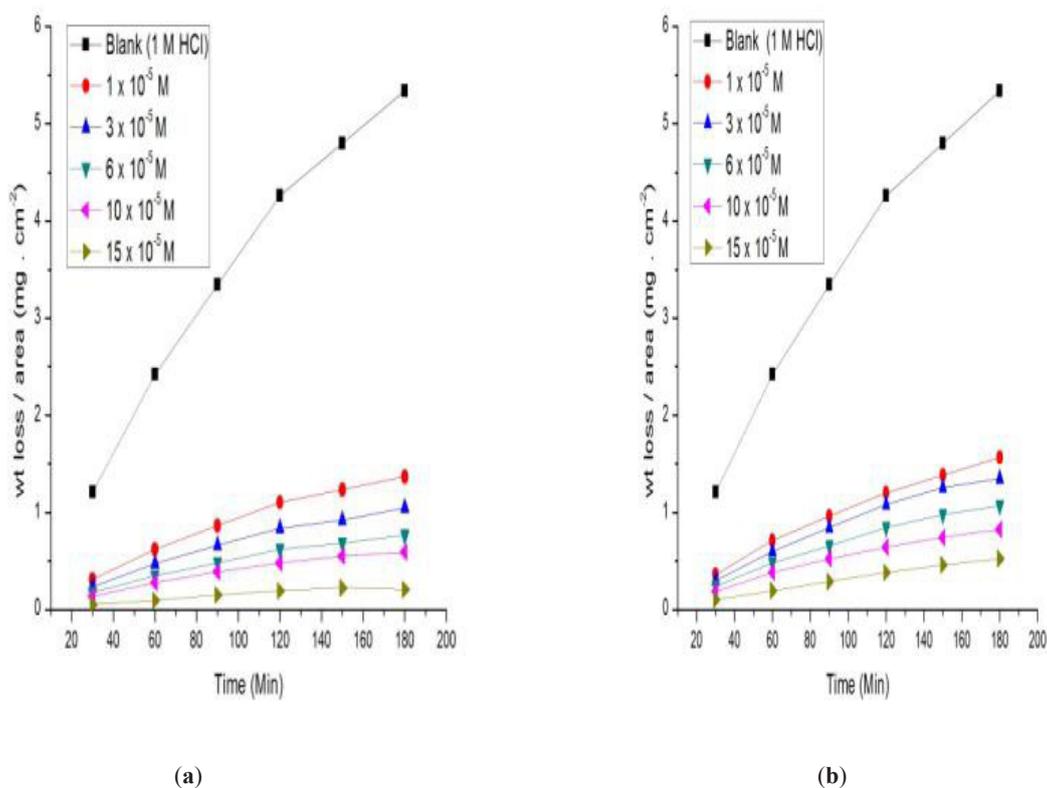| Comp.	Conc., x 10⁻⁵ M	i_{corr} μA cm⁻²	β_c mV dec⁻¹	β_a mV dec⁻¹	C.R mpy	CF-2	CF-3	θ	IE_{EFM}%
Blank	**0**	913.3	149	132	420.8	1.9	3.34	--	--
	1	535.4	103	97	246.7	1.86	2.88	0.414	41.4
	3	522.7	106	98	240.8	1.85	2.2	0.428	42.8
A	**6**	408	59	50	188	2.01	2.19	0.553	55.3
	10	338.7	97	92	156	1.37	2.37	0.629	62.9
	15	222.7	100	97	102.6	1.88	2.6	0.756	75.6

(a)　　　　　　　　　　　　　　　　　　　　(b)

Fig. 6. Weight loss-time curves for the corrosion of C-steel in 1 MHCl in the absence and presence of different concentrations of inhibitors: (a) Corrosion Inhibitor (A); (b) Corrosion Inhibitor (B).

TABLE 9. Weight-loss measurements, inhibition efficiencies (%IE), surface coverage (θ) of inhibitors and corrosion rates data for carbon steel in 1.0 M HCl in the absence and presence of various concentrations of the investigated inhibitors, at 25 °C.

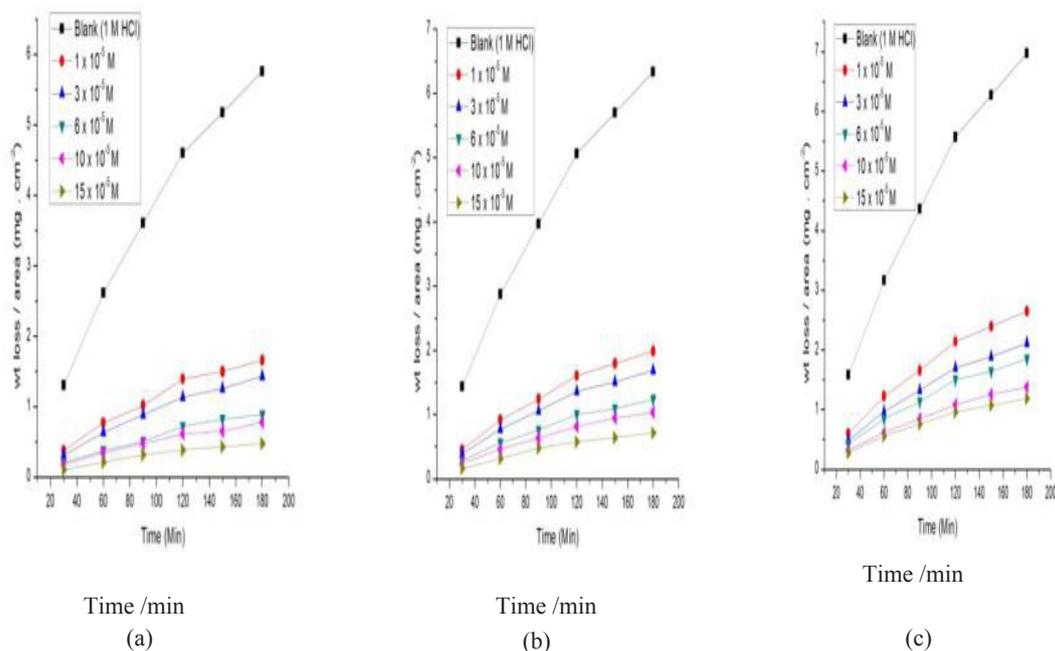| Compound	Conc., x 10^{-5} M	weight loss mg cm^{-2}	% IE	θ	$k_{corr.}$ mg cm^{-2} min^{-1}
1 M HCl	Blank	4.26	---	---	0.036
	1	1.10	74.14	0.74	0.009
	3	0.84	80.34	0.80	0.007
A	6	0.62	85.43	0.85	0.005
	10	0.48	88.76	0.88	0.004
	15	0.19	95.51	0.95	0.002
	1	1.60	62.41	0.62	0.0134
	3	1.57	63.19	0.63	0.0131
B	6	1.37	67.89	0.67	0.0114
	10	1.10	74.24	0.74	0.0091
	15	0.79	81.52	0.81	0.0066

A.M.NEGM *et al.*

Fig. 7. Weight loss-time curves for the corrosion of C-steel in 1 M HCl in the absence and presence of different concentrations of inhibitor (A) at different temperatures: (a) 35 ^{0}C; (b) 45 ^{0}C; (C) 55 ^{0}C.
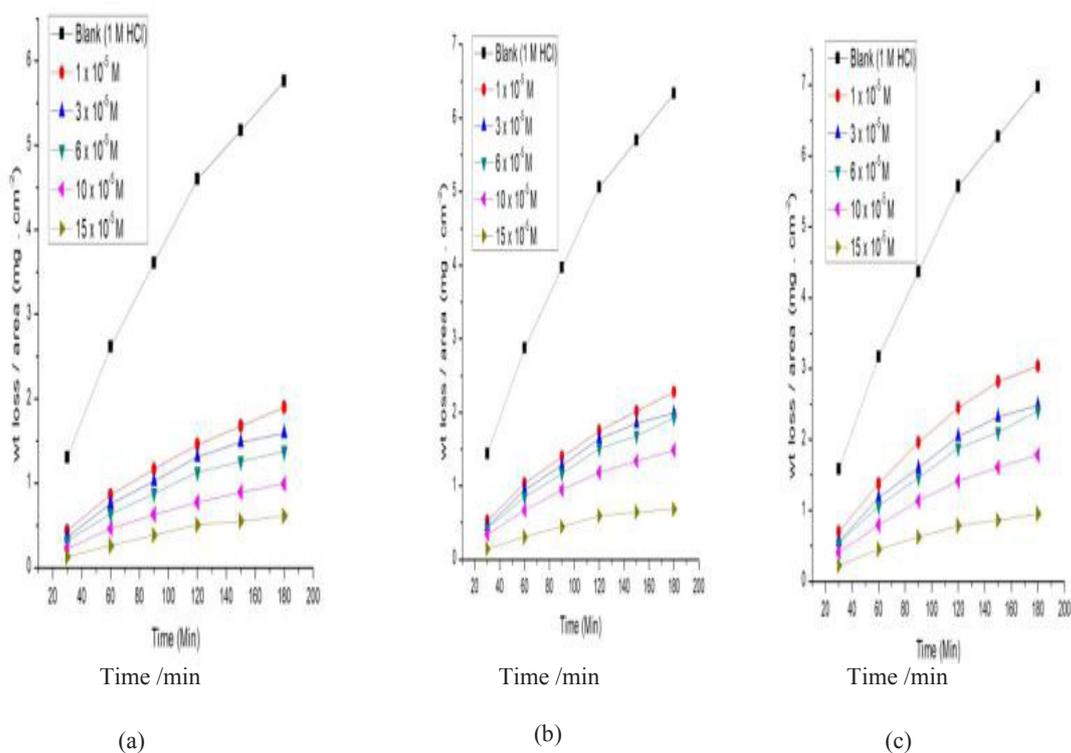

Fig. 8. Weight loss-time curves for the corrosion of C-steel in 1 M HCl in the absence and presence of different concentrations of inhibitor (B) at different temperatures: (a) 35 ^{0}C; (b) 45 ^{0}C; (c) 55 ^{0}C.

TABLE 10. Weight-loss measurements, inhibition efficiencies (%IE), surface coverage (θ) of inhibitors and corrosion rates data for carbon steel in 1.0 M HCl in the absence and presence of various concentrations of the investigated inhibitors, at different temperatures.

Compound		A	B	A	B	A	B	A	B
Temp. °C	Conc., x 10^{-5} M	weight loss mg cm^{-2}		% IE		θ		$k_{corr.}$ mg cm^{-2} min^{-1}	
	Blank	4.26	4.26	---	---	---	--	0.036	0.036
	1	1.1	1.6	74.14	62.41	0.74	0.6241	0.009	0.0134
	3	0.84	1.57	80.34	63.19	0.8	0.6319	0.007	0.0131
25	6	0.62	1.37	85.43	67.89	0.85	0.6789	0.005	0.0114
	10	0.48	1.1	88.76	74.24	0.88	0.7424	0.004	0.0091
	15	0.19	0.79	95.51	81.52	0.95	0.8152	0.002	0.0066
	Blank	4.6	4.6	--		--	--	0.0383	0.0383
	1	1.36	2.02	70.54	56.03	0.7	0.5603	0.0113	0.0169
	3	1.13	1.9	75.37	58.67	0.75	0.5867	0.0094	0.0158
35	6	0.76	1.64	83.55	64.29	0.83	0.6429	0.0063	0.0137
	10	0.61	1.32	86.72	71.36	0.86	0.7136	0.0051	0.011
	15	0.4	1.1	91.25	76.02	0.91	0.7602	0.0034	0.0092
	Blank	5.06	5.06	--		--	--	0.0422	0.0422
	1	1.66	2.33	67.27	53.88	0.67	0.5388	0.0138	0.0195
	3	1.42	2.28	72.01	54.91	0.72	0.5491	0.0118	0.019
45	6	1.09	2.3	78.54	54.55	0.78	0.5455	0.009	0.0192
	10	0.81	1.76	83.91	65.29	0.83	0.6529	0.0068	0.0146
	15	0.6	1.65	88.07	67.3	0.88	0.673	0.005	0.0138
	Blank	5.57	5.57	--		--	--	0.0464	0.0464
	1	2.21	3.11	60.32	44.09	0.6	0.4409	0.0184	0.0259
	3	1.77	2.93	68.19	47.3	0.68	0.473	0.0148	0.0244
55	6	1.63	2.76	70.74	50.42	0.7	0.5042	0.0136	0.023
	10	1.09	2.63	80.49	52.67	0.8	0.5267	0.009	0.022
	15	0.96	2.48	82.77	55.41	0.82	0.5541	0.008	0.0207

The harmonic and intermodulation peaks are clearly visible and are much larger than the background noise. The two large peaks, with amplitude of about 200 μA, are the response to the 40 and 100mHz (2 and 5 Hz) excitation frequencies. It is important to note that between the peaks there is nearly no current response (<100 nA). The experimental EFM data were treated using two different models: complete diffusion control of the cathodic reaction and the "activation" model. For the latter, a set of three nonlinear equations had been solved, assuming that the corrosion potential does not change due to the polarization of the working electrode [22]. The larger peaks were used to calculate the corrosion current density (i_{corr}), the Tafel slopes (β_a & β_c), and the causality factors (CF-2 and CF-3). These electrochemical parameters were listed in Table 8.

The data presented in Table 8 obviously show that the addition of any one of tested compounds at a given concentration to the acidic solution decreases the corrosion current density, indicating that these compounds inhibit the corrosion of carbon steel in 1M HCl through adsorption. The inhibition efficiencies increase by increasing the inhibitor concentrations.

Chemical Measurements (Weight Loss)
  Concentration Effect
Figure 6 exhibits the weight loss-time curves

for the dissolution of carbon steel with and without different concentrations of studied compounds (A&B) in the corrosive solution (1.0 M HCl) at 25 °C. Results in Fig. 6 reveal that, with increasing the concentration, the weight loss decreases and consequently, the corrosion rate decreases as listed in Table 9. The decreasing in weight loss of coupon is mainly due to increasing the adsorption of investigated compounds on carbon steel surface and the adsorption represents a protecting layer and consequently, the coverage surface area (θ) increases. This adsorbed layer minimizes the contact between the metal surface and the acid solution, so decreasing the deadly effectiveness of corrosive solution on the metal surface.

This adsorption can be simply clarified by an electrostatic interaction between positive center in heterocyclic compounds and cathodic sites on the metallic surface [23].

Effect of temperature
The influence of temperature on the corrosion rate for carbon steel in the temperature range 25–55 °C and aggressive solution 1.0 M HCl consisting of various concentrations from the synthesized

compounds, was studied by weight loss method as depicted in Table 10. From the listed data, it is manifest that, upon raising the temperature of the solution, the rate of corrosion increases quickly in the absence of tested inhibitors.

Increasing the solution temperature, accelerate the electrochemical reactions. Therefore, the reacted species are activated; consequently the corrosion reaction takes place quickly. By raising the solution temperature in the presence of inhibitors as shown in Fig. 7& 8. The corrosion inhibition efficiency decreasing as an indication on lowering the surface coverage area by the investigated compounds throughout adsorption on the metal surface. This trend refers to physical adsorption of the tested compounds on the carbon steel surface where is some physical adsorption[24].

According to the results which get from weight loss, potentiodynamic polarization, electrochemical impedance spectroscopy (EIS) measurements and electrochemical frequency modulation (EFM) support the assumption that corrosion inhibition primarily takes place through adsorption of the inhibitors on the C-steel surface. Agreement among
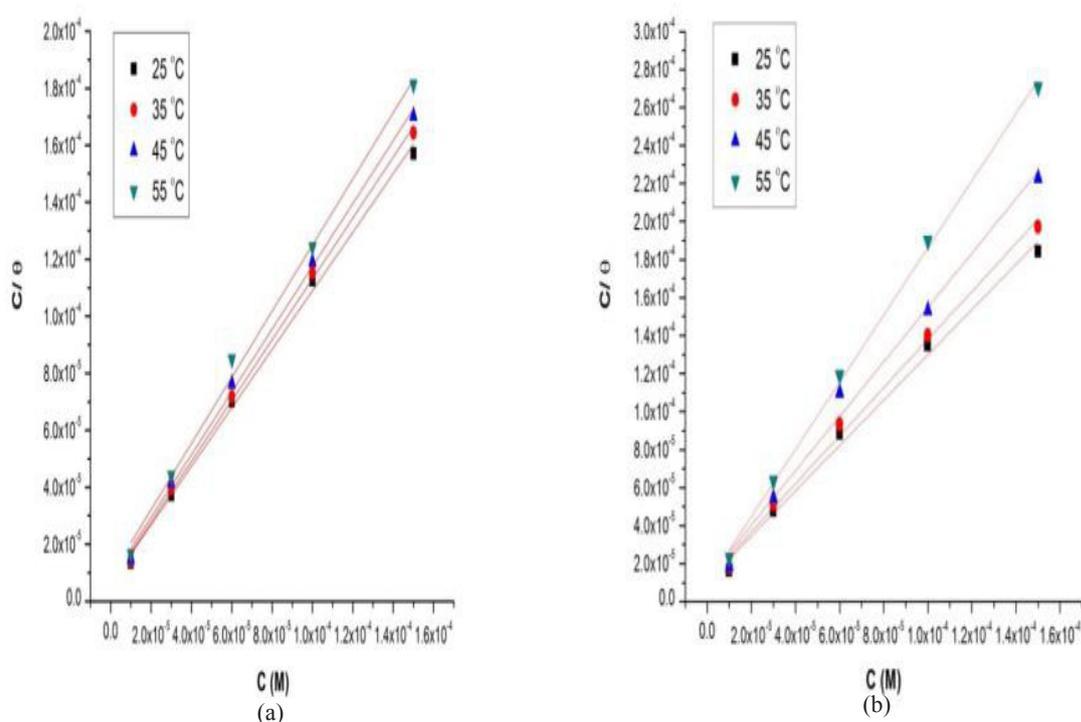

Fig. 9. Langmuir adsorption isotherm on C-steel surface in 1 M HCl at different temperatures: (a) Corrosion Inhibitor (A); (b) Corrosion Inhibitor

TABLE 11. Parameters for Langmuir adsorption isotherm of the investigated inhibitors in 1.0 M HCl on the carbon steel, at different temperatures.

Compound	Temperature ^0C	K_{ads} X 10^5 M^{-1}	Intercept X 10^5	Slope	R^2	$\Delta G^{\circ}_{ads.}$ kJ mol^{-1}	$\Delta H^{\circ}_{ads.}$ kJ mol^{-1}	$\Delta S^{\circ}_{ads.}$ kJ mol^{-1}
A	25	1.59	0.72	1.027	0.996	-39.64		0.12
	35	1.57	0.86	1.067	0.998	-40.92		0.12
	45	1.36	1.15	1.102	0.997	-41.87	-3.44	0.12
	55	1.12	1.45	1.161	0.995	-42.66		0.12
B	25	0.94	1.07	1.192	0.99	-38.32		0.12
	35	0.88	1.14	1.265	0.994	-39.44		0.12
	45	0.85	1.17	1.431	0.988	-40.65	-3.06	0.12
	55	0.83	1.20	1.767	0.998	-41.85		0.12

Table 12. Thermodynamic activation parameters for the decay of carbon steel in 1.0 M HCl with and without presence of various concentrations of the investigated inhibitors.

Compound	$C_{inh.}$ x10^{-5} M	E_a^* kJ mol^{-1}	ΔH^* kJ mol^{-1}	ΔS^* kJ mol^{-1}
Blank	I M HCl	7.27	4.67	-199.66
A	1	18.53	14.71	-177.19
	3	20.08	17.55	-170.24
	6	26.33	20.38	-163.28
	10	34.52	30.19	-134.84
	15	42.72	40.01	-106.4
B	1	17.31	14.71	-188.02
	3	18.56	15.97	-176.39
	6	19.82	17.22	-167.11
	10	23.56	20.96	-156.73
	15	31.22	28.62	-133.52

these different independent techniques indicates the validity of the obtained results.

Adsorption isotherm

One of the most proper methods of describing the adsorption quantitatively is by determining the adsorption isotherm that depicts the metal/inhibitor/environment system [25]. The (θ) obtained from the weight loss technique has been used to fit various adsorption isotherm types and the correlation coefficient (R^2) was utilized to select the best isotherm. The Langmuir isotherm was detected to be the preferable isotherm depict

the adsorption process of studied compounds on carbon steel surface in 1.0 M aggressive solution (HCl) as clarified by the following Equation(10) [26]:

$$\frac{C}{\theta} = \left(\frac{1}{K_{ads}}\right) + C \tag{10}$$

where, C is the inhibitor concentration and K_{ads} is the equilibrium constant of adsorption. Plot of (C/θ) vs. (C) of the studied inhibitors is outlined in Fig. 9. Straight line's relationships for the studied inhibitors were acquired. The values of equilibrium constant (K_{ads}) were listed in Table 11. It is obvious that, the large values of K_{ads}
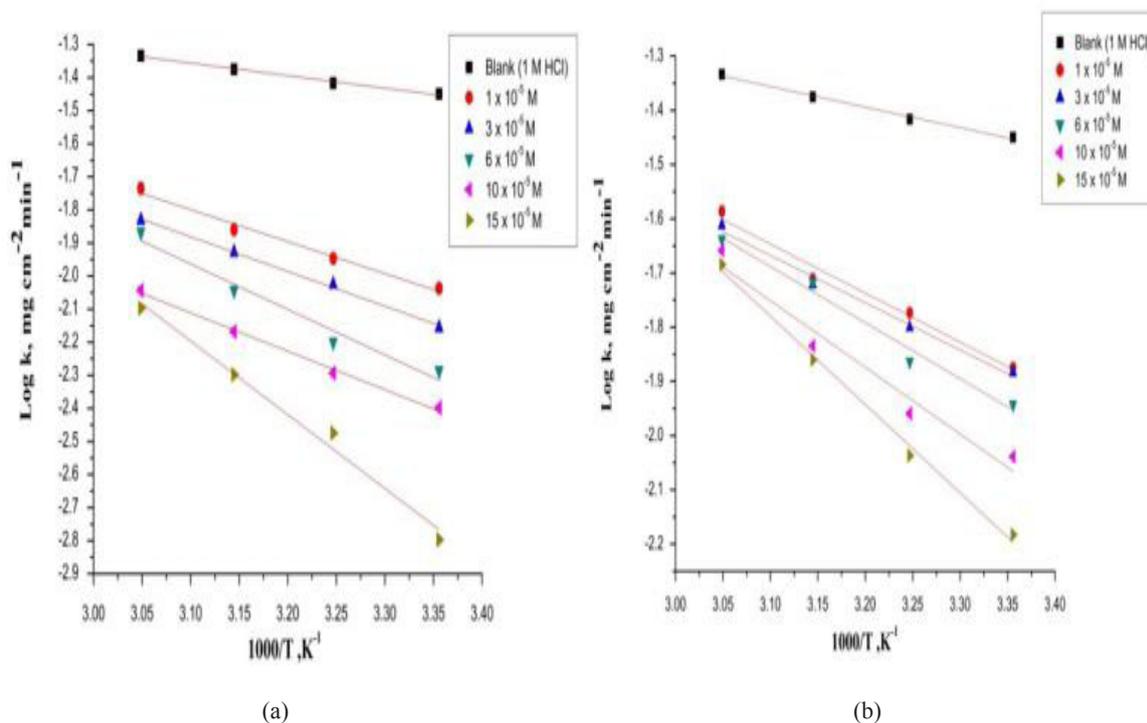
Fig. 10. Arrhenius plots for C-steel corrosion rates (kcorr.) after 120 minutes of immersion in 1 M HCl in the absence and presence of various concentrations of inhibitors: (a) Corrosion Inhibitor (A); (b) Corrosion Inhibitor (B).
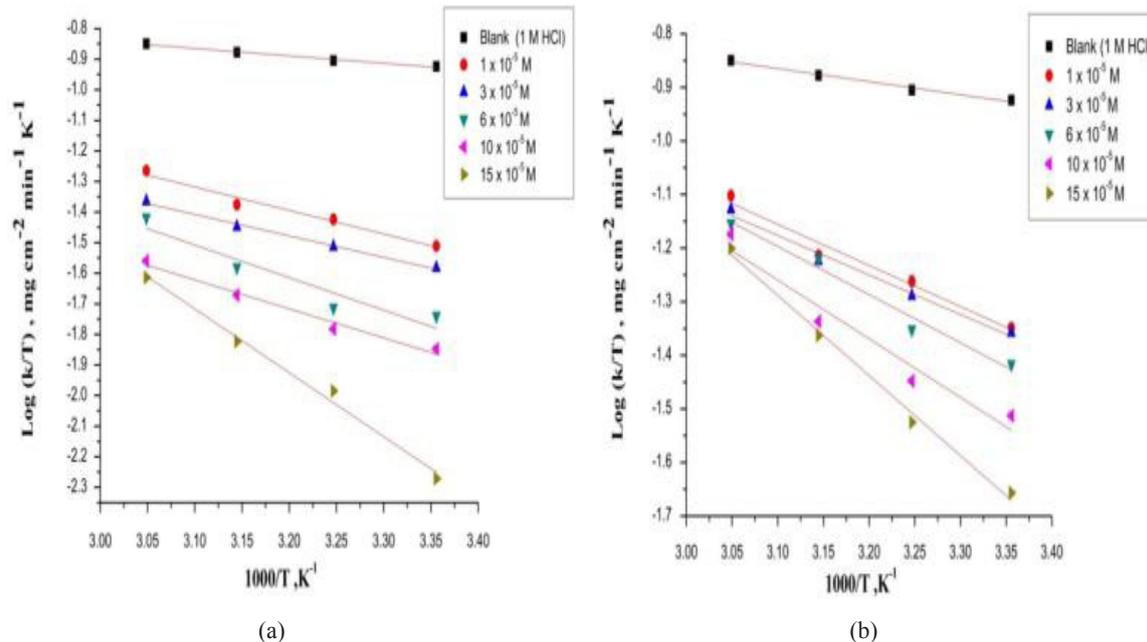

Fig. 11. Transition-state plots for C-steel corrosion rates (kcorr.) after 120 minutes of immersion in 1 M HCl in the absence and presence of various concentrations of inhibitors: (a) Corrosion Inhibitor (A); (b) Corrosion Inhibitor (B).

expressed vigorous adsorption of the considered inhibitors on the surface of carbon steel. Table 11 declared that, by elevating the temperature in range 25–55 °C, the equilibrium constant (K_{ads}) were increasing. Consequently, the process of adsorption by studied inhibitors on the carbon steel surface in corrosive medium considers a physical adsorption.

The adsorption free energy ($\Delta G°_{ads}$) obtained according to the Equation(11) [27]:

$$\Delta G°_{ads} = - R T \ln 55.5 \, K_{ads} \quad (11)$$

where, the value of 55.5 is the molar concentration (mol. L^{-1}) of water in the solution.

The Van't Hoff Equation (12) was used to determine the heat of adsorption (ΔH_{ads}) [28]:

$$\ln K_{ads} = \left(\frac{-\Delta H°_{ads}}{RT}\right) + Constant \quad (12)$$

where,($-\Delta H°_{ads}$ / RT) is the straight-line slope ($\ln K_{ads}$ vs. 1/T), T is absolute temperature and R is gas constant. The standard adsorption entropy ($\Delta S°_{ads}$) calculated through Equation[29]:

$$\Delta G°_{ads} = \Delta H°_{ads} - T \Delta S°_{ads} \quad (13)$$

The calculated thermodynamic parameters, belong the inhibitors adsorption on the carbon steel, were depicted in Table 11. Inspection of the obtained data, it was found that:

The negative values of $\Delta G°_{ads}$ reflect that the adsorption of studied compounds on C- steel surface from 1 M HCl solution is spontaneous process.

$\Delta G°_{ads}$ values decrease (become more negative) with an increase of temperature which indicates the occurrence of exothermic process at which adsorption was favorable with increasing reaction temperature as the result of the inhibitor adsorption on the steel surface.

Generally, values of $\Delta G°_{ads}$ around -20 kJ mol^{-1} or lower are consistent with the electrostatic interaction between the charged molecules and the charged metal (physisorption);those around -40 kJ mol^{-1} or higher involves charge sharing or transfer from organic molecules to the metal surface to form a coordinate type of bond (chemisorption). The calculated $\Delta G°_{ads}$ values are closer to -40 kJ mol^{-1} but it dos not have high differential values and this illustrated by the adsorption mechanism of these molecules

on steel involved two types of interactions, chemisorption and physisorption. The unshared electron pairs in sulphur, nitrogen as well as in oxygen may interact with d-orbitals of iron to provide a protective chemisorbed film beside the physical interaction between the metal and the studied compounds due to the differential of electrostatic charge that cause physisorption.

The values of thermodynamic parameter for the adsorption of inhibitors can provide valuable information about the mechanism of corrosion inhibition. While an endothermic adsorption process ($\Delta H°_{ads} > 0$) is attributed unequivocally to chemisorption, an exothermic adsorption process ($\Delta H°_{ads} < 0$) may involve either physisorption or chemisorption or mixture of both processes. In the presented case, the calculated values of $\Delta H°_{ads}$ for the adsorption of inhibitors in 1 M HCl indicating that this inhibitor is exothermic and may be mixture of both adsorption.

The $\Delta S°_{ads}$ values in the presence of inhibitors in 1 M HCl are positive. The positive sign of $\Delta S°_{ads}$ arises from substitution process, which can be attributed to the increase in the solvent entropy and more positive water desorption entropy.

Activation of thermodynamic parameters

The apparent activation energy E_a^*, the enthalpy of activation ΔH^* and the entropy of activation ΔS^* for the corrosion of C-steel in 1M HCl solutions in the absence and presence of different concentrations of investigated compounds at 25-55 °C was calculated from Arrhenius –type equation (14) &(15) [30]:

$$Rate (k) = A \exp (-E_a^* / RT) \quad (14)$$

$$\log k_{corr.} = \log A - E_a^* / 2.303 \, RT \quad (15)$$

and transition – state equation (16)[31]:

$$Rate (k_{corr}) = RT/ Nh \exp (\Delta S^*/R) \exp (-\Delta H^*/RT) \quad (16)$$

where (A) is the Arrhenius pre-exponential factor. A plot of *log* k_{corr} versus *1/T* gave straight lines as shown in Fig. 10. The enthalpy of activation (ΔH^*) and the entropy of activation (ΔS^*) for the intermediate complex were obtained by applying the transition-state equation (17)[31]:

$$\log (k_{corr}/T) = [\log (R/Nh) + ((\Delta S^*/ 2.303R) - (\Delta H^*/ 2.303RT)] \quad (17)$$
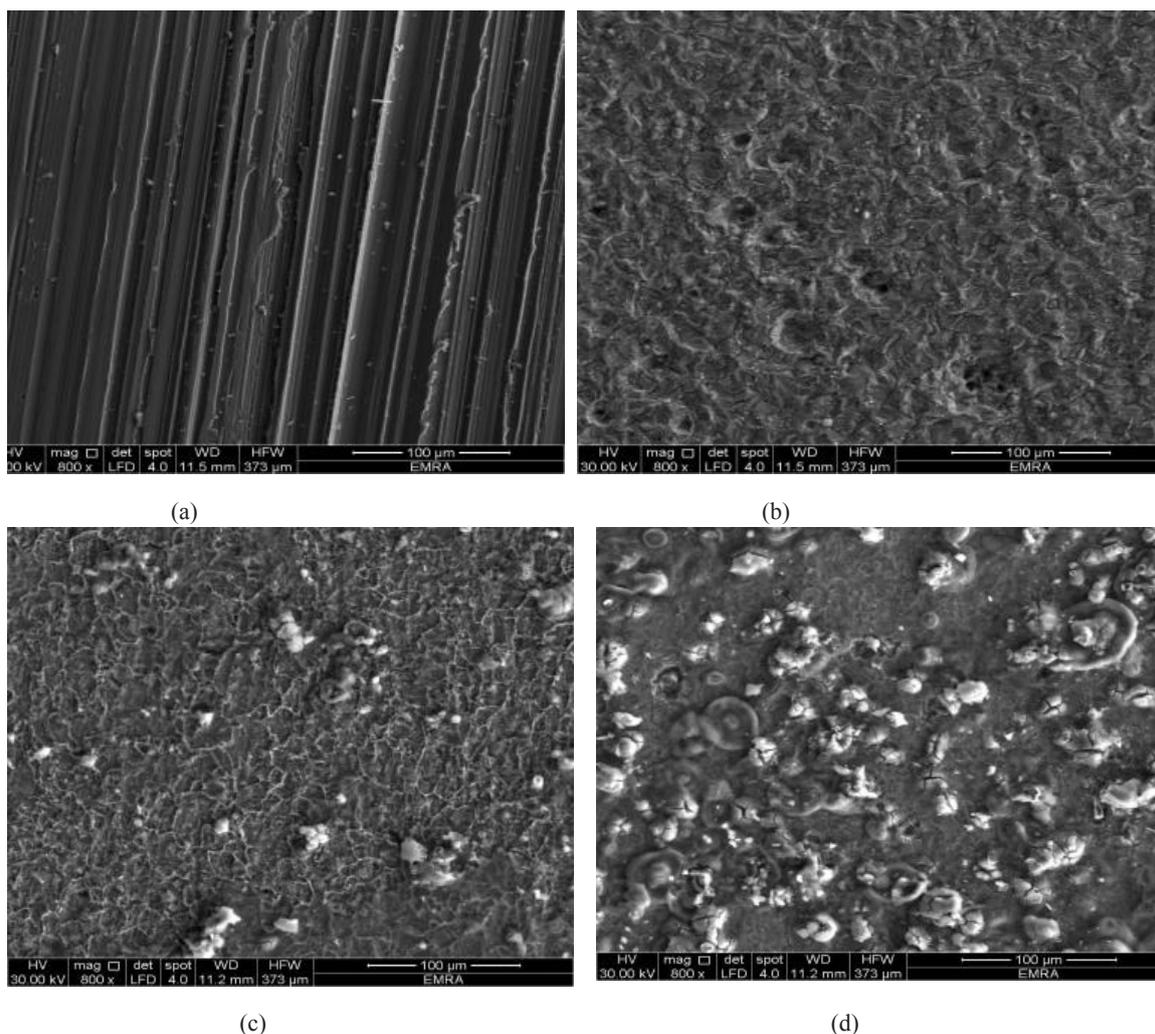
where h is the planck's constant and N is the

Fig. 12. SEM micrographs of C-Steel: (a) C-Steel freshly polished with abrasive paper, degreased with ethanol, and washed by de-mineralized water ; (b) C-Steel immersed for 300 min in an aerated 1 M HCl solution without any additives; (c) C-Steel immersed for 300 min in an aerated 1 M HCl solution containing 15 x 10^{-5} M of inhibitor A; (d) C-Steel immersed for 300 min in an aerated 1 M HCl solution containing 15 x 10^{-5} M of inhibitor B.

Avogadro's number. A plot of *log (k_{corr}/T)* versus *1/T* should give a straight line (Fig. 11) with a slope of *(-ΔH*/ 2.303R)* and an intercept of *[log (R/Nh) + (ΔS*/ 2.303R)]* from which the values of *ΔH** and *ΔS** were calculated, respectively. All estimated kinetic-thermodynamic parameters were tabulated in Table 12.

From the results of Table12. it is clear that the presence of investigated compounds modified the values of the apparently increased activation energies. The values of the activation energy determined for blank acid and acid with various concentrations of organic derivatives are listed in Table 12. The addition of the inhibitor modified the values of the apparent activation energies.

It was found that values for inhibited systems in the acid media increased with the increasing concentration of inhibitor which was higher than those for uninhibited system. This was indicative of higher energy barrier formed by the studied organic derivatives towards the corrosion reaction. The E_a^* values are helpful to determine the type of adsorption. In the case of chemisorption, the E_a^* values are greater than 80 kJmol^{-1} whereas in this case of chemisorption they are lesser than 80kJmol^{-1}. This suggests that physical mode of adsorption had occurred due to the interaction between the studied organic derivatives and C-steel surface which suggests that these organic derivatives are sensitive to reaction temperatures [32].
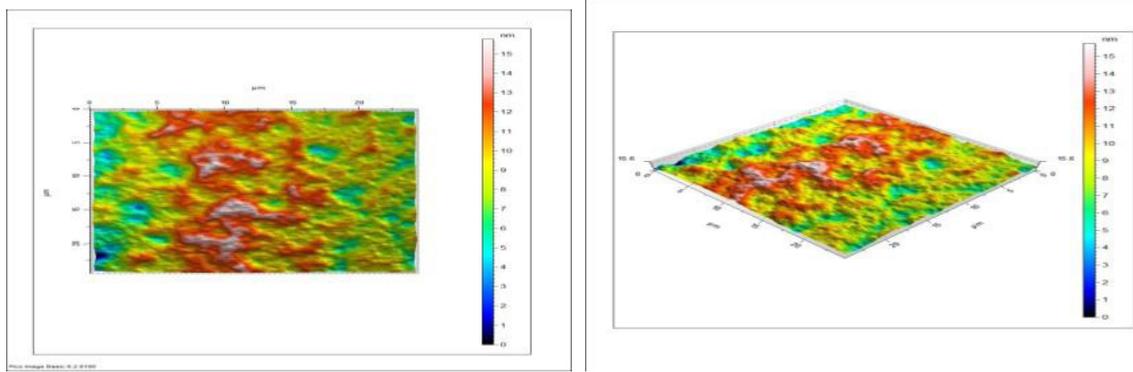
(a)

(b)

Fig. 13. The *AFM* photographs of carbon steel surface in 1 M HCl aggressive solution after immersion for 48 hours (left is 2D; right is 3D).
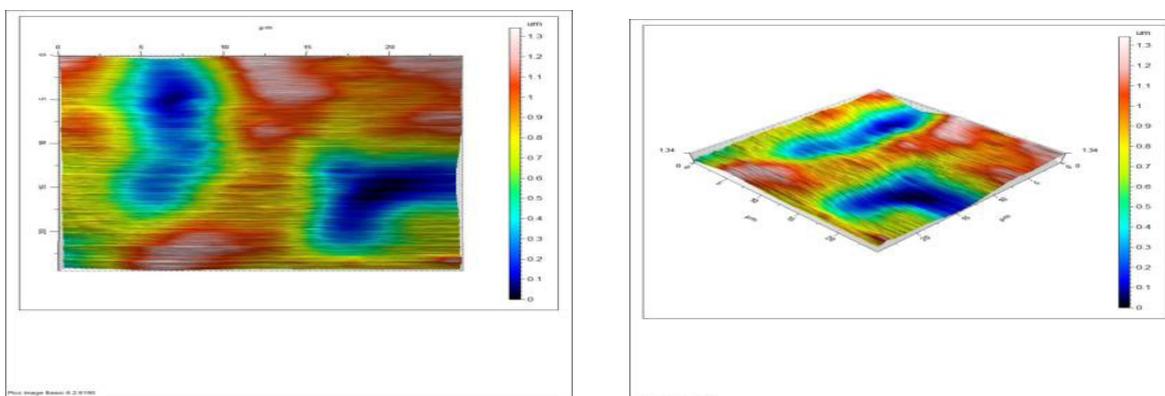

(a)

(b)

Fig. 14. The *AFM* photographs of carbon steel surface in 1 M HCl aggressive solution containing 15x10⁻⁵ M of inhibitor (A)after immersion for 48 hours(left is 2D; right is 3D).
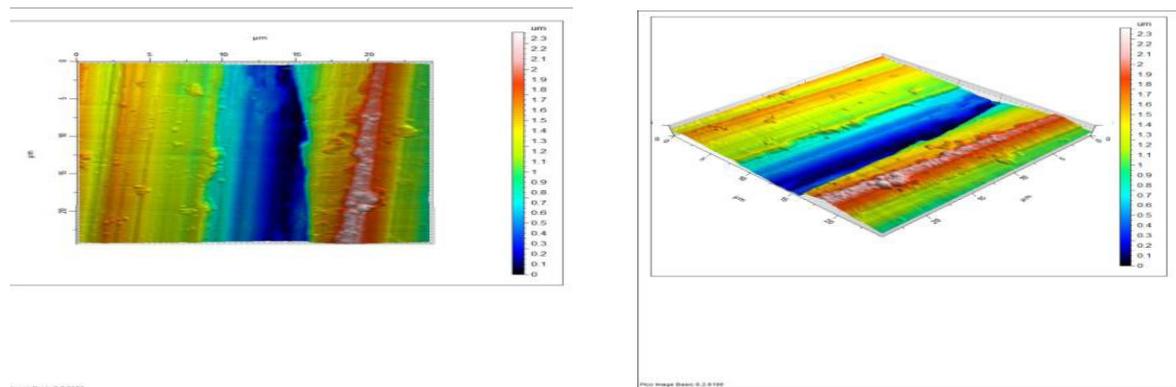

(a)

(b)

Fig. 15. The AFM photographs of carbon steel surface in 1 M HCl aggressive solution containing 15x10⁻⁵ M of inhibitor (B)after immersion for 48 hours(left is 2D; right is 3D).

From the above discussion, it is clear that the addition of organic derivatives modified the values of E_a^* which is due to adsorption [33] on C-steel surface. This leads to the formation of species which then inhibit the anodic dissolution of C-steel, supporting the physisorption mechanism. On the other hand, chemisorption which arise due to the interaction of aromatic rings, nitrogen and oxygen atoms with Fe present in C-steel and can not be ignored.

The positive signs of ΔH^* reflect the endothermic nature of the steel dissolution process. Large and negative values of ΔS^* imply that the activated complex in the rate determining step represents an association rather than dissociation step, meaning that decrease in disordering takes place ongoing from reactants to the activated complex.

Surface morphology
Scanning Electron Microscopy (SEM) technique
Figure 12 clarified the carbon steel specimens micrographic with and without the existence of 15x 10^{-5} M from the synthesized compounds after exposure for 2 days immersion in 1.0 M aggressive medium (HCl). It is apparent that, the blank specimen surface of the carbon steel afford from severe corrosion offensive, but the surface in the existence of the synthesized compounds were silky and minimal affected by the process of corrosion than the blank. Due to the adsorption of molecules on the carbon steel surface and made a preservative layer on the surface, the surface became isolated by the formed layer of the synthesized inhibitors from the corrosive medium and so the synthesized compounds is an effective inhibitor under the studied conditions [34].

Atomic Force Microscopy (AFM) analysis
The surface morphology at nano-to micro-scale was assessed by AFM which consider a spectacular and creative method for studying the impact of inhibitors on the corrosion generation at the carbon steel/solution interface. Figures 13, 14&15 depict the morphologies of carbon steel specimens after immersion for 5 h in 1 M HCl solutions without and with the absence of inhibitors; the surface displayed a very irregular topography due to corrosion attack. The average roughness R_a of steel in 1M HCl solution without inhibitor was calculated as 65.6 nm by atomic force microscopy. In

the presence of inhibitors A and B, smoother surface was obtained and the R_a value decreased to 0.96 and 2.21 nm as a consequence of low corrosion damage and the protective formation of an inhibitor layer on steel surface. It can be clearly observed that in the absence of inhibitor, the steel surface was seriously corroded with areas of uniform corrosion. In the presence of inhibitors, however, the specimen surface was smoother as shown in Fig. 14 & 15. This is due to the involvement of inhibitor molecules in the interaction with the reaction sites of steel surface, resulting in a decrease in the contact between iron and the aggressive medium and sequentially exhibited excellent inhibition effect[35]:

References

1. Wang, E., Guo, Y., Yang, L., Han, M., Zhao, J. and Cheng, X., Nanomaterials as sorbents to remove heavy metal ions in wastewater treatment. *J. Environ. Anal. Toxicol.* **2**, 2-7 (2010).

2. Kumari, M., Pittman, Jr.C.U. and Mohan, D., Heavy metals [chromium (VI) and lead (II)] removal from water using mesoporous magnetite (Fe3O4) nanospheres. *J. Colloid Interface Sci.* **442**, 120-132 (2015).

3. Chowdhury, S.R. and Yanful, E.K., Kinetics of cadmium (II) uptake by mixed maghemite magnetite nanoparticles. *J. Environ. Manage.* **129**, 642-651 (2013).

4. Chowdhury, S.R. and Yanful, E.K. Arsenic and chromium removal by mixed magnetite–maghemite nanoparticles and the effect of phosphate on removal. *J. Environ. Manage.* **91**, 2238-2247 (2010).

5. Ahmed, M.A., Ali, S.M., El-Deka, S.I. and Galal, A., Magnetite–hematite nanoparticles prepared by green methods for heavy metal ions removal from water. *Mater. Sci. Eng.* **B178**, 744-751 (2013).

6. Cullity, B.D., *Elements Of X-Rays Diffraction.* Wiley, USA (1978).

7. Boparai, H.K., Joseph, M. and O'Carroll, D. M., Kinetics and thermodynamics of cadmium ion removal by adsorption onto nanozerovalent iron particles. *J. Hazard. Mater.* **186**, 458–465 (2011).

8. Praveen, B.M. and Venkatesha, T.V., *Int. J.Electrochem. Sci.* **4**, 267–275 (2009).

9. Asefi, D., Arami, M., Sarabi, A.A. and Mahmoodi, N.M., *Corros. Sci.* **51**, 1817–1821 (2009).

10. Moura, E.F., Neto, A.O.W., Dantas, T.N.C., Junior and Gurgel, H.S., *Colloids Surf. A: Physicochem. Eng. Aspects*, **340**, 199–207 (2009).

11. Branzoi, V., Branzoi, F. and Baibarac, M., *Mater. Chem. Phys.* **65**, 288 (2000).

12. Atkin, R., Craig, V.S.J., Wanless, E.J. and Biggs, S., *Adv. Coll. Int. Sci.* **103**, 219 (2003).

13. Poorqasemi, E., Abootalebi, O., Peikari, M. and Haqdar, F., *Corros. Sci.* **51,** 1043–1054 (2009).

14. Elachouri, M., Hajji, M.S., Kertit, S., Essassi, E.M., Salem, M. and Coudert, R., *Corros. Sci.* **37**, 381–389 (1995).

15. Kurihara, M.; Yamamura, H.; Nakanishi, T. High recovery/high pressure membranes for brine conversion SWRO process development and its performance data. *Desalination.* **125**, 9–15 (1999).

16. Wei, Q.; McGovern, R.; Lienhard, J. Two-stage reverse osmosis: Optimal element configuration and energy savings. In *Proceedings of the IDA World Congress* **51**, 1043–1054 (2009).

17. Hegazy, M.A., Badawi, A.M., Abd El Rehim, S.S. and Kamel, W., *Corros. Sci.* **69**, 110–122 (2012).

18. Takeshita, T. I., Wakebe and Maeda, S., *J. Am. Oil Chem. Soc.* **59**, 90 (1982).

19. Shuichi, M., Kazayasu, I., Sadao, Y., Kazuo, K. and Tsuyoshi, Y., *J. Am. Oil Chem. Soc.* **67**, 996 – 100 (1991).

20. Rosen, M. J. "*Surfactants and Interfacial Phenomena*", Wiley, New York, **72** (1987).

21. ASTM G1-72, Practice for preparing, cleaning and evaluating corrosion test specimens, (1990).

22. Benabdellah, M., Touzani, R., Dafali, A., Hammouti, B. and Kadiri, S.E., *Mater. Lett.* **61,** 1197 (2007).

23. Lebrini, M., Lagrenée, M., Vezin, H., Traisnel, M. and Bentiss, F., *Corros. Sci.* **49,** 2254 (2007).

24. Scendo, M., *Corros. Sci.* **49**, 373 (2007).

25. Oguzie, E.E., Li, Y. and Wang, F.H., *J. Coll. Interf. Sci.* **310**, 90 (2007).

26. Villamil, R.F.V., Corio, P., Rubin, J.C. and Agostinho, S.M.L., *J. Electroanal. Chem.* **535**, 75 (2002).

27. Emad A.Badr, *J. Industrial and Engineering Chemistry*, **20**, 3361-3366 (2014).

28. Lebrini, M., Lagrenée, M., Traisnel, M., Gengembre, L., Vezin, H. and Bentiss, F., *Appl. Surf. Sci.* **253**, 9267–9276 (2007).

29. Safak, S., Duran, B., Yurt, A. and Turkogˇlu, G., *Corros. Sci.* **54**, 251–259 (2012).

30. Bensajjay, F., Alehyen, S., El Achouri, M. and Kertit, S., *Anti-Corros. Methods Mater.* **50**, 402 (2003).

31. Mu, G., Li, X. and Liu, G., *Corros. Sci.* **47**, 1932 (2005).

32. El-Sherbini, Foad, E.E., Abd-El-Wahab, S.M. and Deyab, M.A., *Mater. Chem. Phys.* **82**, 631 (2003).

33. Bentiss, F., Lebrini, M. and Lagrenée, M., *Corros. Sci.* **47**, 2915–2931 (2005).

34. Khaled, K.F., *Electrochimica Acta,* **48**, 2493– 2503 (2003).

35. Behpour, M., Ghoreishi, S.M., Soltani, N., Salavati-Niasari, M. and Hamadanian, M., A Gandomi, *Corros. Sci.* **50**, 2172–2181 (2008).

دراسة سلوك التآكل لمواسير دوائر التبريد بعد استخدام المياه العادمة من محطات التناضح العكسي كمصدر مياه مغذى و ذلك بعد اضافة مركبات جديدة مشتقة من الاستان و استخدامها كمثبطات للتآكل

عبدالله مصطفى نجم¹، عبدالعزيزالسيد فودة²، سعد عبدالوهاب محمد³، تريز البير يوسف³، رباب شلوف²

¹شركة القاهرة للانتاج الكهربي ـ الجيزة ـ مصر.

²قسم الكيمياء ـ كلية العلوم ـ جامعة المنصورة ـ المنصورة ـ مصر.

³قسم الكيمياء ـ كلية العلوم ـ جامعة عين شمس ـ القاهرة ـ مصر.

مشكلة التآكل من المشاكل التي تواجه العالم منذ زمن بعيد و حتى الآن حيث انه لا يمكن منع التآكل نهائيا و لكن يمكن تقليل مخاطرة على الفلزات و السبائك التى تصنع منها خطوط الانابيب المستخدمة فى نقل المياه و جميع السوائل و من المعروف أن المياه من المصادر المتجددة، ولكن الواقع يقول إن كميات المياه تتناقص في ظل تزايد الطلب عليها، وأصبح تقليل تكلفة انتاج المتر المكعب من المياه المستخدمة فى الصناعات تحدياً كبيراً بالنسبة إلى دول العالم، ما يستوجب التفكير في إعادة وضع استراتيجيات جديدة لإدارة المياه في الصناعات، خصوصا أن العديد من اقتصاديات العالم ستتأثر مستقبلاً بمدى جودة إدارتها لاستهلاكها المائي، و هذه الدراسة تربط بين اعادة استخدام المياه وفى نفس الوقت حماية خطوط الانابيب ولذلك تناقش تآكل خطوط الأنابيب المصنوعة من الصلب الكربونى بعد اعادة استخدام المياه العادمة من محطات تحلية المياه باستخدام التناضح العكسي في حامض الهيدروكلويك و كيفية حمايته.

وقد استخدمت طرق كيميائية و كهروكيميائية للتعرف على تاثير المركبات الجديدة كما انه تم فحص السطح عن طريق الميكروسكوب الالكترونى و مجهرة القوة الذرية و قد اكدت الدراسة على وجود انهيار سطح الصلب الكربونى فى عدم وجود المثبطات نتيجة عملية التآكل وتكوين طبقة على سطح الصلب الكربونى فى وجود المثبطات.